CHAPTER - 3

EXPERIMENTAL METHODS

In the present experimental work a series of measurements of coherent differential scattering cross sections of gamma ray photons has been made employing a wide range of photon energies from 84.30 KeV to 2 MeV and target atoms representing low, medium and high Z atoms. These measurements have been divided into two parts with regard to the angle of scattering. The range of momentum transfer covered in these measurements is between 0.01 mc and 10 mc. Two different experimental set-ups have been used, one meant for scattering angles from 1° to 25° and the other from 30° - 150°. In both these arrangements the experiments consisted essentially in detecting the scattered photons from the scatterer placed in the path of a well collimated beam of gamma ray photons emitted from a gamma ray source placed in a property shielded housing. Experimental arrangements for both small and large angle scattering will be described separately. A brief description of the gamma ray sources, scatterer materials used are given below. The gamma ray sources were procured from Isotope Division, Bhaba Atomic Research Centre, Trombay, INDIA. The scatterer materials used were 99.99% pure chemically.

3.1 Radioactive sources

Nos.	Source	Strength	Photon energy	Half life
1.	Thallium-170	100 mCi	84.30 KeV	127d
2.	Cerium-141	100 mCi	145.00 KeV	32.5d
3.	Mercury-203	20 mCi	280 KeV	47d
4.	Caesium-137	20 mCi	662 KeV	30y
5.	Zinc-65	100 mCi	1.115 MeV	245d
6.	Cobalt-60	300 mCi	1.17 and 1.33 MeV	5.27y
7.	Antimony-124	810 mCi	1.70 and 2.09 MeV	60d.

3.2 Targets

Nos.	Target element	Atomic number	Form
1.	Boron	5	Boron Carbide and Boron Nitride powder
2.	Carbon	6	Powder
3.	Nitrogen	7	Boron Nitride powder
4.	Aluminium	13	Metallic plate and cylinder
5.	Sulphur	16	Powder

Contd..

Nos.	Target element	Atomic number	Form
6.	Copper	29	Metallic plate and cylinder
7.	Silver	47	Metallic plate
8.	Lanthanum	57	Lanthanum Oxide powder
9.	Neodymium	60	Neodymium oxide powder
10.	Samarium	62	Samarium oxide powder
11.	Dysprosium	66	Dysprosium oxide powder
12.	Gold	79	Metallic plate
13.	Mercury	80	Metallic liquid
14.	Lead	82	Metallic plate and cylinder
15.	Thorium	90	Thorium nitrate powder
16.	Uranium	92	Uranium oxide powder.

For low angle measurements annular scatterers were cut out from thin pure metal sheets. Values of inner and outer radii of these rings varied from 2.36 c.m to 3.37 c.m and from 3.67 c.m to 4.64 c.m respectively. Their thicknesses varied from 0.12 m.m to 0.3 m.m. Target materials in the form of powders were tightly packed in

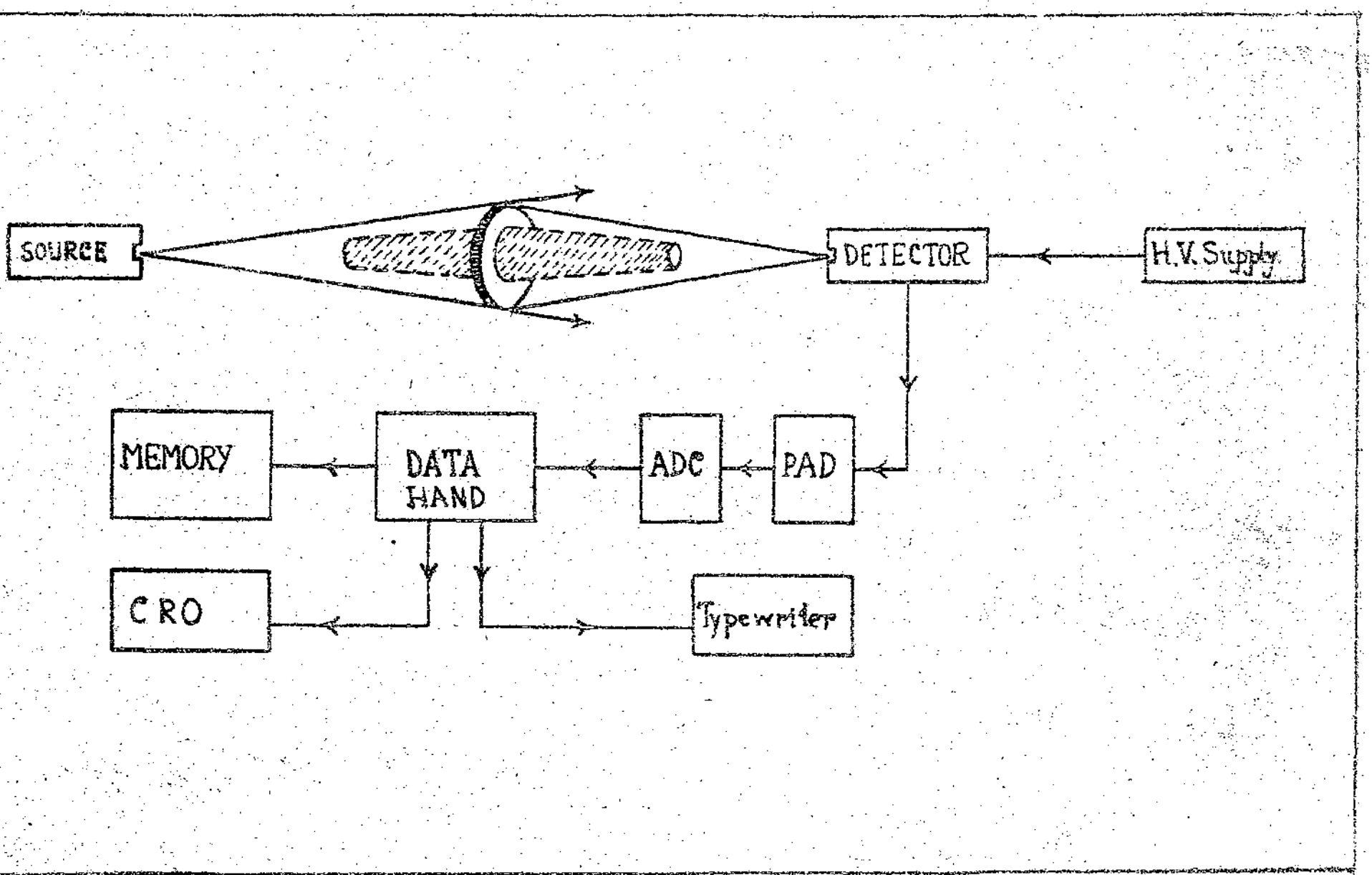

Fig. 6. EXPERIMENTAL ARRANGEMENT (SMALL ANGLE SCATTERING)

thin annular perpex cases. For large angle measurements the scatterers were either cylindrical in shape of radii between 0.75 m.m and 9 m.m or rectangular plates of dimension 7.5 c.m x 7.5 c.m x 0.35 c.m.

3.3 Experimental arrangement for small angle measurements

The geometry used in the experimental arrangement is shown in the figure 6. A conical beam of gamma ray photons from the source was allowed to strike the scatterer. A double conical cylinder made either of iron or brass was suspended in such a way between the source and the detector that the straight part of the conical beam of gamma rays were effectively absorbed by it and the detector was completely within the shadow of this stopper. This stopper was suspended with the help of thin silk threads tied at both ends. The scatterers in the shape of annular rings were placed as shown in the figure 6.

The range of scattering angles was varied by varying with the radii of the annular rings or the distances between the source and the scatterer and scatterer and the detector. The source and the detector were properly shielded to minimize background counts. Except for the double cone stopper, the air mass and the suspension threads

of the double cone stopper, there was no background material within the geometry of the experimental set-up.

At a scattering angle θ the expression for the total number of photons N_s scattered per unit time is given by

$$N_S = \frac{N_0}{4\pi R^2} \epsilon N_{at} \frac{d\sigma(\theta)}{d\Omega} \Omega_1 \exp\left(-\frac{\mu t}{\cos\phi}\right) \quad \ldots (3.3.1)$$

where

N_s = Number of photons emitted by the main source per unit time.

r = the mean source to scatterer distance.

N_{at} = the total number of atoms in the effective volume of the scatterer.

Ω_1 = the solid angle subtended by the detector at the scatterer.

μ = the attenuation co-efficient of the target material (taken from Hubbell[47])

t = the thickness of the scatterer.

ϕ = the mean angle between the lines joining the source to the scatterer and to the detector.

The detector efficiency ϵ and the solid angle Ω_1 subtended by the detector at the scatterer were eliminated from eqn. (3.3.1) by a short comparison run with a weaker reference source of the same photon energy placed at the position of the scatter. Then eqn. (3.3.1) becomes

$$\frac{d\sigma(\theta)}{d\Omega} = \frac{N_S}{N_{ref.}} \frac{r^2}{S} \frac{1}{N_{at.}} \exp\left(\frac{\mu t}{\cos\phi}\right) \quad \ldots (3.3.2)$$

where N_{ref} is the number of ref counts from a weak reference source placed at the position of the scatterer and S is the strength of the main source relative to the weak reference source.

The thickness of a particular scatterer was found by measuring the inner and outer radii of the annular scatterer and accurately weighing the scatterer. Narrow beam transmission experiment was also carried out with Caesium-137 source to measure the thickness and to check the uniformity of packing of the target materials in the form of powder in perspex cases.

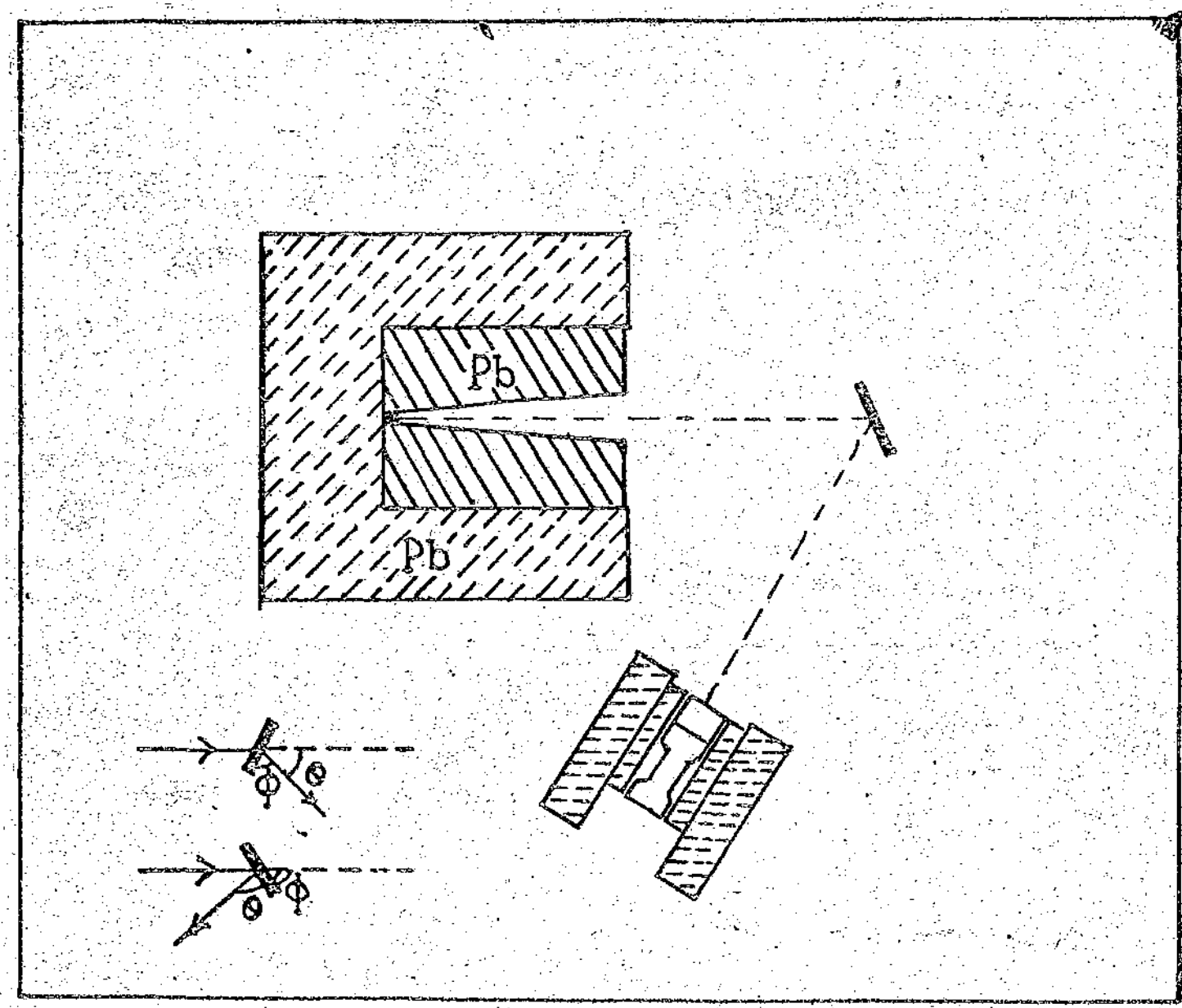

Fig.7. Experimental arrangement. (Large angle scatt.)

3.4 Large angle scattering

Experimental arrangement for measuring differential cross section at scattering angles 30^0 - 165^0 is shown in the figure 7. A high degree of collimation of the primary photon beam was obtained by using proper shielding of the source. A conical bore was made through the axis of a solid lead cylinder of radius 6 c.m and length 15 c.m. The gamma ray source encapsulated in a cylindrical capsule was pushed in the rear hole of this conical bore. An elaborate shielding on all sides of this cylinder was made with the help of some old lead bricks. The exit radius of the bore was such that a uniform collimated beam of gamma ray photons might strike all parts of the targets placed at the required position. Various source to scatterer and scatterer to detector distances were used depending on the energy and intensity of the sources to obtain a good statistical accuracy of the recorded scattered counts. But in each case the source to scatterer and scatterer to detector distances were kept almost similar. Those distances varied from 15 c.m to 50 c.m. When using scatterers of plate geometry scattered counts were detected in the reflection geometry for scattering angles greater than 90^0 and for scattering angles less than 90^0 transmission

geometry was used. To minimise the spread of the scattering angle δ, due to finite size of the scatterer the angle δ' between the plane of the scatterer and the direction of the incident photon beam φ was found out from the following relation (Fig. 2).

$$\frac{r}{R} = \frac{\sin\phi}{\sin(\theta-\phi)} \qquad \ldots (3.4.1)$$

where r is the distance between the source and the target, R is the distance between target and the detector when using scatterers in the shape of right circular cylinder the maximum solid angle between the scatterer and the detector was 5×10^{-2} sr and the corresponding spread of the scattering angle was generally small.

In the case of scatterer of plate geometry the differential scattering cross section is given by

$$\frac{d\sigma}{d\Omega} = \frac{N_s}{N_{ref}} \frac{1}{S} \frac{r^2}{N_{at} G(\theta)} \qquad \ldots (3.4.2)$$

where

N_s = total number of scattered photons under the photopeak per unit time.

N_{ref} = total number of counts from a weak reference source of the same energy placed at the position of scatterer.

S = strength of the strong source relative to the weaker one.

r = distance between source and the scatterer.

N_{at} = number of target atoms in the target materials.

$Q(\theta)$ = correction for absorption of the incident and scattered photons in the scatterer found out ~~the~~ from the following relation of Kahane et al[48]

$$G(\theta) = \frac{e^{-\mu t/\sin(\phi-\theta)}}{\mu t\left(\frac{1}{\sin\phi} - \frac{1}{\sin(\theta-\phi)}\right)}\left[1 - e^{-\mu t\left(\frac{1}{\sin\phi} - \frac{1}{\sin(\theta-\phi)}\right)}\right]$$

for transmission geometry

and

$$G_x(\theta) = \frac{1 - e^{-\mu t\left(\frac{1}{\sin\phi} - \frac{1}{\sin(\theta-\phi)}\right)}}{\mu t\left(\frac{1}{\sin\phi} - \frac{1}{\sin(\theta-\phi)}\right)}$$

for reflection geometry

When experiments were carried out with monochromatic sources and cylindrical scatterers, the coherent scattering cross sections were found out by comparing coherent component peak with the incoherent peak of the same spectrum. The coherent scattering cross section is given by

$$\frac{\frac{d\sigma}{d\Omega}_{coh}}{\frac{d\sigma}{d\Omega}_{incoh}} = \frac{(I_x(\theta,\eta))_{coh} \cdot f_{sx}(\theta,\eta)\epsilon_2}{(I_x(\theta,\eta))_{incoh} f_{px}(\theta,\eta)\epsilon_1}$$

... (3.4.5)

where $(I_x(\theta,r))_{coh}$ and $(I_x(\theta,r))_{incoh}$ are the scattered intensities (photopeak area of the coherent and incoherent spectrum at an angle θ from any cylindrical scatterer X of radius r, $f_{sx}(\theta,r)$ is the attenuation factor for the incoherently scattered photons, $f_{px}(\theta,r)$ is the absorption factor for the coherently scattered photons and $\frac{d\sigma}{d\Omega}_{incoh}$ is the incoherent scattering cross section, calculated using the equation

$$\frac{d\sigma}{d\Omega}_{incoh} = d\sigma(\theta)_{KN} S(q,Z) \quad \ldots (3.4.6)$$

ϵ_1 and ϵ_2 are the photopeak efficiencies of the detector for coherently and incoherently scattered photons. In the above method the shape of the incoherent peak in the main scattered spectrum was always referred to that in the comparison scattered spectrum from Aluminium scatterer of same dimension.

3.5 Measurements

Before starting the experiment proper with a particular radio isotope the multichannel analyser (ND 1100) channels were calibrated. Two types of NaI (Tl) detectors were used for the present measurements. It was either a 7.5 x 7.5 c.m crystal mounted on RCA 8054 photomultiplier tube or a 1" x 1" crystal mounted on RCA 6199 photomultiplier tube. The high voltage supply to the photomultiplier tube was provided from the highly stabilized output from solid state high voltage power supply manufactured by ECIL.

The calibration of the M.C.A. channels was done by using Co-57 (122 KeV), Ba-133 (0.36 MeV), Cs-137 (0.662 MeV), Mn-54 (0.84 MeV) and Co-60 (1.173, 1.332 MeV) reference sources. The high voltage supply, preamplifier (PAD) gain and the zero level control of the ADC were adjusted to get a good linearity of the calibration curve passing through the zero channel for a particular setting of the conversion gain of the ADC. In most of the measurements 512 channels were used. A direct spectrum of a particular source was then recorded for a particular preset live time of the M.C.A. The detector was placed at a suitable distance from the source so as to avoid "dead time loss". The experimental source was then removed and a similar weaker

reference source emitting photons of the same energy as that of the experimental one was placed at the position of the strong source. Again a direct spectrum was recorded for the same duration of time. While using a strong source emitting high energy photons, all the first 256 channels were shifted. In this way the ADC was relieved of analysing photons of lower energies and consequently "dead time loss" was avoided. As both the spectra accumulated were from sources emitting the same photon energy and placed at the same position with respect to the detector, the ratios of the counts under the photo peaks of these spectra would directly give the relative ratio of the strengths of the strong source with respect to the weaker one after careful subtraction of counts recorded under these photo peaks due to various disturbances. These ratios for different isotopes were also checked by the strengths of these sources furnished by the Isotope Division, BARC.

Before placing the strong experimental source at the rear hole of the conical bore as mentioned earlier, the position of the scatterer in the large angle measurements and the alignment of the stopper in the small angle measurements were checked with the help of a telescope placed behind the rear hole and viewing through the conical bore. After placing the source and removing the target,

and placing the detector in position, the shielding of the source and detector was checked and the background counts were kept to a minimum by placing extra shielding materials wherever needed. Then counts were recorded in the following sequence for large angle measurements, (i) with the scatterer in such a position that the detector did not see it but the incident photon beam struck it, (ii) with the scatterer not in line with the source but in front of the detector and (iii) without the scatterer. The procedure was repeated for all scattering angles for which measurements were made. In all the three cases the background remained practically the same indicating that the effect of the contribution of the scatterer dependent background was negligibly small. For small angle measurements some scatterer dependent backgrounds were noticed. A method of correction for this will be described later.

For both small and large angle measurements a trial run for a short period of time was made to detect the scattered counts, with the scatterer placed in the proper position. After subtracting the background counts with the scatterer removed an approximate idea about the duration of time required to acquire counts for a satisfactory statistical accuracy was estimated. First of all,

the background counts were recorded in the add mode for the predetermined time with the scatterer removed. The data stored in the core memory of the M.C.A were then typed out. Though a direct subtraction of the background could be made by the M.C.A itself, it was not done to allow us to correct any shift in the channels during the long time the data were acquired. After typing out the data for the background the memory contents were erased and a fresh run for the same duration of time was made to acquire data for the scattered counts together with the background, with the scatterer in position. The pre set live time of acquire varied, in the present set of measurements from 10 K Sec to 100 K Sec. The constancy in the calibration of the channels was checked after each set of run. The whole experiment was carried out in a big air conditioned room keeping the room temperature fixed at 20^{0}C.

3.6 Errors and corrections

A number of corrections are needed to minimise certain systematic errors resulting from the following reasons in the measurements described. These are stated below.

1) In the measurement of source to scatterer, scatterer to detector distances, scattering angles,

thicknesses of the scatterers, attenuation co-efficients of scatterers etc. Great care was taken to measure the linear distances and errors limited to within 1.0 m.m. In the case of small angle scattering, the mean scattering angle was found out from the geometry of the experimental set up by knowing the source to scatterer, scatterer to detector distances and inner and outer radii of the annular ring scatterers. As the differential cross section is strongly dependent on small scattering angles, all these parameters were measured with great accuracy. As the scatterer-detector distances were large in the case of small angle measurements, the solid angles subtended by the detector were relatively very small. The maximum fractional solid angle from the detector, a 1" x 1" detector head was 1×10^{-3}. The errors in the measurement of small angles were restricted to within 6 min.

2) Variation of background in the presence and absence of scatterers in small angle measurements was found in the following way. The scatterer sample could change the detector background through absorption of some photons in it. The amount B_s of sample dependent background absorbed in the sample is given by $\sim B_s (1-e^{-\mu t})$. By taking measurements at two scatterer thicknesses, B_s was found out

and the correction for the absorbed fraction of the background was obtained. In the symmetrical scattering arrangement (Fig. 6) the photons multiply scattered towards and away from the detector should be mutually compensated to a great extent, therefore, the effect of multiple scattering may be neglected as very thin scatterers were used.

3) Uncertainty in the spectrum analysis due to presence of various disturbing effects in the coherent photo peak.

There are various effects which contribute to the pulse height distribution which are not desired in the scattered spectrum. Before an analysis was made of the scattered spectrum all these effects were recognised and taken into account. The intensity of coherently scattered spectrum is related to the number of counts under the full energy peak. The full energy peak has a Gaussian shape of the form

$$G(x) = \frac{1}{\sqrt{2\pi}\sigma} \exp\left[-(x-x_0)^2/2\sigma^2\right] \quad \ldots (3.6.1)$$

where χ_0 is the midpoint and σ is a width parameter. The total counts due to coherent scattering at small angles were found by subtracting incoherently scattered photons determined theoretically by using HFHF scattering factors.

There was not much difficulty in finding the shape of coherent scattered spectra in most of the measurements, especially when monoenergetic sources were used and for large angle scattering where coherent and incoherent peaks were all separated. The following technique was adopted when using multiple energy sources or when the coherent and incoherent peaks were close to each other. A weak reference source, emitting photons of same energy as that of a particular experimental source energy as that of a particular experimental source was placed at the position of the scatterer and counts recorded. The shape of this recorded spectrum was obtained after subtracting backgrounds and other disturbing effects. The parameters of the Gaussian in (3.6.1) were found out. There was no difficulty in finding the peaks of the coherently scattered photons which should fall in the same channel as obtained with direct spectra. The parameters determined from the Gaussian of the direct spectrum were used and a least square fit of the observed counts detected under the scattered photo peak was made to obtain the coherent

scattered spectra. The least square fit programme was made and executed with the help of a D.C.M micro computer. One difficulty arises due to presence of Compton scattered photons from bound electrons of the scatterer.

The maximum energy of these Compton scattered photons from bound electrons of target atoms may go upto to the incident photon energy minus the binding energies of these electrons. We have done some measurements[49] of the differential scattering cross section as a function of energy of the incoherent scattering of photons ($\frac{d^2\sigma}{d\Omega dE}$) from bound electrons of different target atoms using several photon energies. A very simple fast coincidence circuit developed by the author[50] was used to gate the A.D.C. of the M.C.A. In addition to the main detector detecting scattered counts from the target, another detector (1/2" x 1½" mounted on RCA 6342 was used to detect the X-ray photons resulting from vacancies created by Compton scattering off bound electrons. Two different pre-amplifiers (PAD) were used for the two detectors. The discriminators of PAD 1 are adjusted to give an output due to pulses of photon energy equal to the K or L-shell binding energies. The PAD 2 was used to receive pulses from the main detector meant for detecting the scattered photons. The output of both PADS were delayed with the

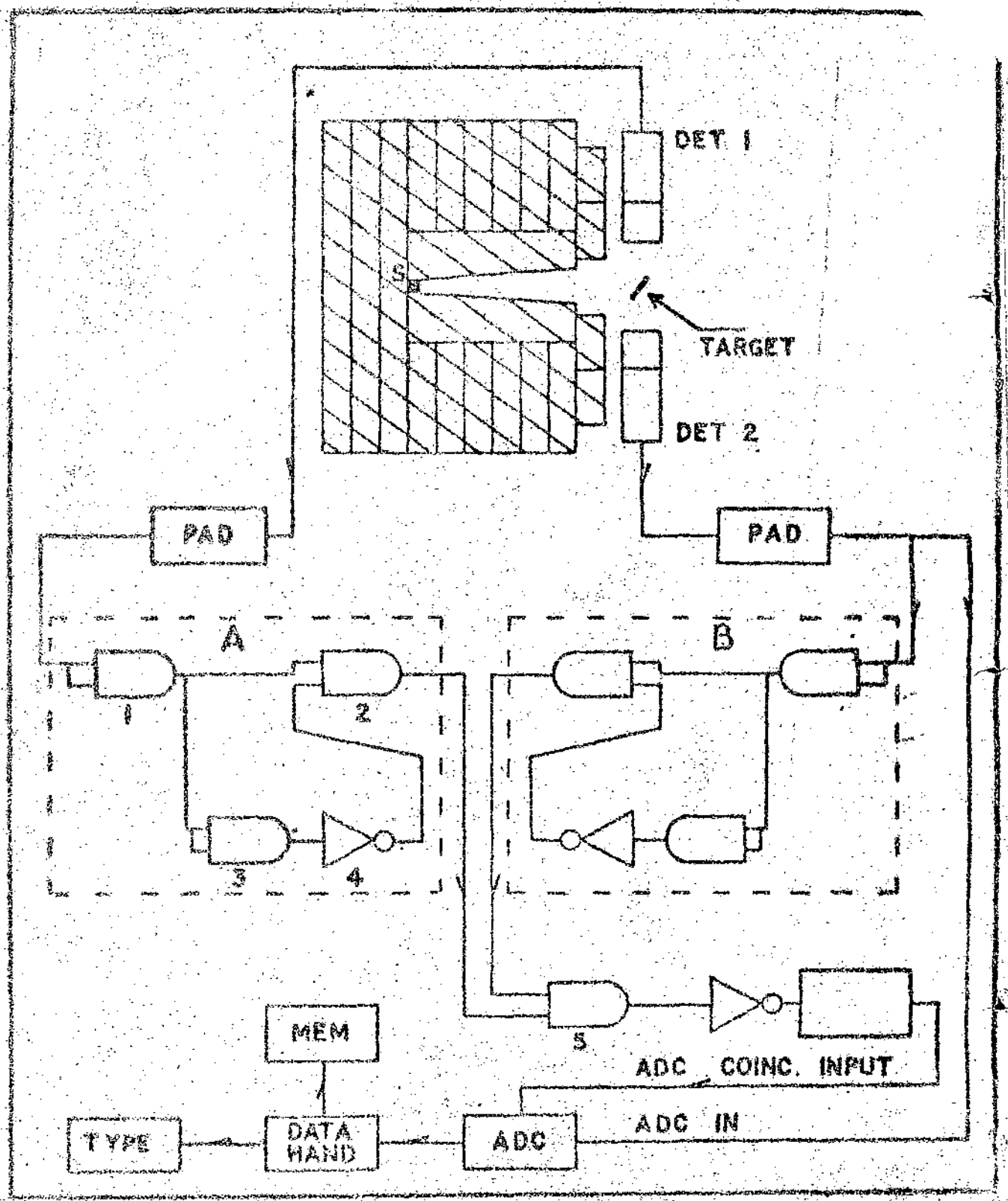
DET 1
TARGET
DET 2
PAD
PAD
A
B
1
2
3
4
5
MEM
ADC COINC. INPUT
TYPE
DATA HAND
ADC
ADC IN

Fig 8.

help of some AND and INVERTER gates as shown in the Fig. 6. These delayed pulses were again fed to the input terminals of an AND gate, so that if the pulses from the two detectors arrived within a time determined by the delay obtained then an output pulse resulted. This coincident output pulse was then fed into a Schmitt trigger IC to have a pulse of proper duration and shape required for the A.D.C coinc. input. When this coincidence input terminal was free, the A.D.C. analysed all pulses received from PAD 2. Now in the presence of this coincidence input the A.D.C analysed only the Compton scattered photons from bound electrons. The number of such photons was found to contribute 10 - 14% to the total counts recorded under the coherent peaks of different target materials and energies used.

3.7 Experimental Results

The experimental results obtained in the present set of measurements are listed in tables 10-12. The figure in the parenthesis indicate errors.

Table 10 Measured Cross Section for Coherent Scattering.

Photon energy (KeV)	Target (Z)	θ	q(mc)	Experimental cross section (b at^{-1} sr^{-1})
84.30	Al(13)	$5^0 26'$	0.0098	6.4200(0.35)
		$4^0 19'$	0.0126	5.322(0.30)
		$5^0 6'$	0.0146	4.998(0.27)
		$9^0 36'$	0.0275	1.722(0.09)
84.30	Zn(29)	$3^0 26'$	0.0098	43.133(0.80)
		$4^0 25'$	0.0126	33.901(0.69)
		$5^0 5'$	0.0157	21.593(0.54)
		$9^0 36'$	0.0275	10.003(0.23)
		$15^0 15'$	0.0436	4.82(0.15)
84.30	Ag(47)	$3^0 27'$	0.0099	121.60(1.73)
		$4^0 29'$	0.0128	78.44(1.55)
		$6^0 34'$	0.0183	50.79(1.06)
		$10^0 40'$	0.0306	35.12(1.93)
		$15^0 22'$	0.0439	19.61(1.07)
84.30	La(57)	$3^0 58'$	0.01138	165.52(3.37)
		$12^0 13'$	0.035	41.53(2.01)

Contd..

Table 10 (Contd..)

Photon energy (KeV)	Target (Z)	θ	q(mc)	Experimental cross section (b $at^{-1}Sr^{-1}$)
84.30	Sn(68)	5°3'	0.0145	143.06(3.98)
		12°13'	0.0350	47.05(1.69)
84.30	Dy(66)	5°57'	0.01153	199.48(3.09)
84.30	Au(79)	2°39'	0.003	382.5(4.2)
		5°04'	0.015	268.9(5.4)
		10°38'	0.030	130.5(2.6)
		15°13'	0.038	92.8(2.9)
		24°12'	0.069	23.3(1.0)
145	Al(13)	1°36'	0.0035	6.68(0.19)
		3°46'	0.019	4.02(0.16)
145	Cu(29)	1°36'	0.0035	48.46(2.66)
		2°49'	0.014	32.81(1.64)
		3°46'	0.019	24.46(0.97)
		8°05'	0.04	6.43(0.25)
		10°06'	0.05	6.01(0.19)
145	Sn(50)	1°56'	0.0035	145.23(4.55)
		2°49'	0.014	103.12(5.09)
		3°46'	0.019	80.16(4.00)
		8°05'	0.04	24.82(1.24)

Table 11 Measured cross section for coherent scattering for Z = 38

Photon energy KeV	θ	q(mc)	Experimental cross section(b at^{-1}Sr^{-1})
145	1°30'	0.009	419.2(12.5)
	2°24'	0.018	287.7(8.1)
	3°46'	0.019	279.7(8.4)
	6°05'	0.049	92.3(4.6)
	13°53'	0.069	54.6(3.2)
	15°46'	0.070	53.1(2.6)
	19°33'	0.098	23.2(2.3)
	24°50'	0.132	13.3(1.2)
350	3°0'	0.019	210.02(±8.2)
	5°44'	0.0328	69.16(± 3.1)
	10°3'	0.1008	17.03(±0.85)
662	1°46'	0.04	85.10(± 1.96)
	3°58'	0.09	25.37(± 0.89)
	4°32'	0.11	12.66(± 0.64)
	10°5'	0.22	2.33(± 0.08)
	14°6'	0.309	0.60(± 0.06)
	30°4'	0.4506	0.209 (±0.03)

Contd..

Table 11 (Contd..)

Photon energy KeV	Q	q(mc)	Experimental cross section(b $at^{-1}Sr^{-1}$)
1170	1^{o}	0.04	110.31(2.4)
	2^{o}	0.079	23.50(1.4)
	$3^{o}03'$	0.128	9.10(0.4)
	$4^{o}11'$	0.188	3.01(0.3)
	$10^{o}5'$	0.401	0.393(±0.02)
	$12^{o}4'$		0.150(±0.006)
1332.5	1^{o}	0.045	82.74 (± 3.2)
	2^{o}	0.09	25.12(± 1.3)
	$10^{o}5'$	0.476	0.210(± 0.08)
	$12^{o}4'$	0.562	0.130(± 0.05)

Table 12 Measured Cross Sections for Coherent Scattering.

Photon energy (KeV)	Target Z	θ	q(mc)	Experimental cross section (b at^{-1} sr^{-1})
662	Cu(29)	1°46'	0.04	4.76(0.16)
		2°38'	0.06	3.68(0.11)
	Sn(50)	1°46'	0.04	84.25(0.59)
		2°30'	0.06	12.82(0.34)
		3°56'	0.09	6.17(0.22)
	La(57)	1°46'	0.04	30.13(0.80)
	Nd(60)	1°46'	0.04	33.64(0.85)
	Dy(66)	1°46'	0.04	41.93(0.96)
	Hg(80)	1°46'	0.04	76.17(1.66)
	Pb(82)	1°46'	0.04	85.10(1.96)
		3°39'	0.09	25.37(0.69)
		4°52'	0.11	18.66(0.44)
	U(90)	1°46'	0.04	104.21(2.60)

Table 13 Measured Cross Section for Coherent Scattering

Photon energy MeV	Target Z	θ	q(mc)	Experimental cross section (mb at-1sr-1)
1.115	Pb(82)	32°	1.20	18.10 0.30
		45°	1.66	2.80 0.20
		60°	2.18	0.61 0.02
		95°	3.21	0.17 0.01
		135°	4.03	0.15 0.02
1.70	Pb(82)	60°	3.32	0.0618(0.0041)
		90°	4.70	0.0571(0.0028)
		105°	5.27	0.0477(0.0027)
		120°	5.76	0.0536(0.0034)
		150°	6.42	0.0638(0.0038)
2.09	Pb(82)	60°	4.09	0.0476(0.0049)
		75°	4.97	0.0403(0.0041)
		90°	5.78	0.0494(0.0049)
		105°	6.48	0.0506(0.0044)
		120°	7.08	0.0476(0.0041)
		150°	7.90	0.0576(0.0047)

Contd..

Table 15 (Contd..)

Photon energy MeV	Target Z	θ	q(mc)	Experimental cross section (mb at^{-1} sr^{-1})
1.70	U(92)	60°	3.32	0.157(0.010)
		90°	4.70	0.102(0.006)
		120°	5.76	0.113(0.0073)
2.00	U(92)	60°	4.09	0.09(0.0038)
		90°	5.78	0.076(0.005)
		120°	7.08	0.078(0.005)